ORIGINAL ARTICLE

Journal of Cachexia, Sarcopenia and Muscle (2017)
Published online in Wiley Online Library (wileyonlinelibrary.com) **DOI:** 10.1002/jcsm.12204

Cardiac troponin T and fast skeletal muscle denervation in ageing

Zherong Xu[1,2†], Xin Feng[3†], Juan Dong[1], Zhong-Min Wang[1], Jingyun Lee[4], Cristina Furdui[4], Daniel Clark Files[5], Kristen M. Beavers[6], Stephen Kritchevsky[1,7], Carolanne Milligan[8], Jian-Ping Jin[9], Osvaldo Delbono[1,7] & Tan Zhang[1,7*]

[1]*Department of Internal Medicine, Section on Gerontology and Geriatric Medicine, Wake Forest School of Medicine, Winston-Salem, NC, 27157, USA;* [2]*Department of Geriatrics, First Affiliated Hospital, Zhejiang University, School of Medicine, Hangzhou, 310003, China;* [3]*Department of Otolaryngology, Wake Forest School of Medicine, Winston-Salem, NC, 27157, USA;* [4]*Department of Internal Medicine, Section on Molecular Medicine, Wake Forest School of Medicine, Winston-Salem, NC, 27157, USA;* [5]*Internal Medicine-Pulmonary, Critical Care, Allergy and Immunology, Gerontology and Geriatric Medicine and the Critical Illness Injury and Recovery Research Center, Wake Forest School of Medicine, Winston-Salem, NC, 27157, USA;* [6]*Department of Health and Exercise Science, Wake Forest University, Winston-Salem, NC, 27109, USA;* [7]*Sticht Center for Healthy Aging and Alzheimer's Prevention, Wake Forest School of Medicine, Winston-Salem, NC, 27157, USA;* [8]*Department of Neurobiology and Anatomy, Wake Forest School of Medicine, Winston-Salem, NC, 27157, USA;* [9]*Department of Physiology, Wayne State University School of Medicine, Detroit, MI, 48201, USA*

Abstract

Background Ageing skeletal muscle undergoes chronic denervation, and the neuromuscular junction (NMJ), the key structure that connects motor neuron nerves with muscle cells, shows increased defects with ageing. Previous studies in various species have shown that with ageing, type II fast-twitch skeletal muscle fibres show more atrophy and NMJ deterioration than type I slow-twitch fibres. However, how this process is regulated is largely unknown. A better understanding of the mechanisms regulating skeletal muscle fibre-type specific denervation at the NMJ could be critical to identifying novel treatments for sarcopenia. Cardiac troponin T (cTnT), the heart muscle-specific isoform of TnT, is a key component of the mechanisms of muscle contraction. It is expressed in skeletal muscle during early development, after acute sciatic nerve denervation, in various neuromuscular diseases and possibly in ageing muscle. Yet the subcellular localization and function of cTnT in skeletal muscle is largely unknown.

Methods Studies were carried out on isolated skeletal muscles from mice, vervet monkeys, and humans. Immunoblotting, immunoprecipitation, and mass spectrometry were used to analyse protein expression, real-time reverse transcription polymerase chain reaction was used to measure gene expression, immunofluorescence staining was performed for subcellular distribution assay of proteins, and electromyographic recording was used to analyse neurotransmission at the NMJ.

Results Levels of cTnT expression in skeletal muscle increased with ageing in mice. In addition, cTnT was highly enriched at the NMJ region—but mainly in the fast-twitch, not the slow-twitch, muscle of old mice. We further found that the protein kinase A (PKA) RIα subunit was largely removed from, while PKA RIIα and RIIβ are enriched at, the NMJ—again, preferentially in fast-twitch but not slow-twitch muscle in old mice. Knocking down cTnT in fast skeletal muscle of old mice: (i) increased PKA RIα and reduced PKA RIIα at the NMJ; (ii) decreased the levels of gene expression of muscle denervation markers; and (iii) enhanced neurotransmission efficiency at NMJ.

Conclusions Cardiac troponin T at the NMJ region contributes to NMJ functional decline with ageing mainly in the fast-twitch skeletal muscle through interfering with PKA signalling. This knowledge could inform useful targets for prevention and therapy of age-related decline in muscle function.

Keywords Cardiac troponin T; Neuromuscular junction; Sarcopenia; Protein kinase A; Denervation

Received: 6 October 2016; Revised: 13 February 2017; Accepted: 1 March 2017
**Correspondence to: Tan Zhang, Department of Internal Medicine, Section on Gerontology and Geriatric Medicine, Wake Forest School of Medicine, Medical Center Boulevard, Winston-Salem NC, 27157, USA. Phone: 336-716-6918; Fax: 336-716-2273, Email: tzhang@wakehealth.edu*
†These two authors contributed equally to this work.

Introduction

Troponin T (TnT) is a key regulator of contractile machinery in the striated muscle. Its physiological role is regulating excitation-contraction coupling by forming a Tn complex with TnI and TnC and interacting with tropomyosin (Tm) and the actin double-stranded filaments in muscle cells.[1] Three TnT isoforms, TnT1, TnT3, and TnT2—encoded by gene *Tnnt1*, *Tnnt3*, and *Tnnt2* genes, respectively—are expressed in slow-twitch and fast-twitch skeletal muscles and cardiac muscle, respectively. Recent and growing evidence shows that TnT may also have some non-classical functions through different subcellular localization and interaction with other molecules. For instance, Tn and Tm are found in the nucleus in various tissues.[2,3] We recently found that fast skeletal muscle TnT3 can function as a transcription regulator that modulates muscle contraction-related gene expression, including calcium channel beta1a and alpha1s subunits, by nuclear translocation.[4,5]

Unlike cardiac TnI, which is highly specific for cardiac muscle, TnT2, the cardiac isoform of troponin T (cTnT), is also expressed in developing skeletal muscles, after sciatic nerve denervation, and in various neuromuscular diseases.[6–8] Whereas injury to myocardium causes the simultaneous release of both cTnI and cTnT into the circulation, denervation and chronic injury of skeletal muscle may induce expression and release of cTnT, but not cTnI, from the skeletal muscle. Therefore, elevated circulating cTnT, but not cTnI, has been found in patients with various neuromuscular diseases and in healthy elderly patients without clinical cardiovascular disease.[7,9]

Cardiac troponin T functions as a dual A-kinase anchoring protein (D-AKAP) that interacts with the protein kinase A (PKA) regulatory subunits RI and RII in the heart muscle.[10] Although PKA RIα, RIIα, and RIIβ are all localized at the postsynaptic neuromuscular junction (NMJ), their patterns differ.[11] The role of RIα in mediating nicotinic acetylcholine receptor (nAChR) stabilization at the postsynaptic NMJ is known, but the role of RIIα and RIIβ at this site is still not clear.[12–15] In addition, whether PKA RIα plays a role in regulation of NMJ stability in a fibre type-specific and age-dependent manner is unknown.

In this study, we tested our hypothesis that levels of cTnT expression in skeletal muscle increase with ageing and may interfere with PKA signalling at NMJ. We found that cTnT is highly enriched at the NMJ region—but mainly in the fast-twitch, not the slow-twitch, muscle of old mice. PKA RIα is largely removed from, while PKA RIIα and RIIβ are enriched at the NMJ—but again, preferentially in fast-twitch but not slow-twitch muscle of old mice. Knocking down cTnT in fast skeletal muscle of old mice (i) increased PKA RIα and reduced PKA RIIα at the NMJ; (ii) decreased the levels of gene expression of muscle denervation markers; and (iii) enhanced neurotransmission efficiency at NMJ. Our findings imply that cTnT contributes to NMJ disorganization and skeletal muscle denervation in ageing through interfering with PKA signalling, mainly in fast-twitch skeletal muscle.

Materials and methods

Reagents and antibodies

Mouse anti-cTnT monoclonal antibody (1C11, 1F11) and rabbit anti-cTnT monoclonal antibody ab125266 were purchased from Abcam (San Diego, CA, USA) and 4B8 generated in laboratory of Dr Jian-Ping Jin (Wayne State University, Detroit, MI, USA), previously shown to be highly specific for cTnT in multiple species without cross reaction to the fast or slow isoforms of TnT.[16] Mouse anti-PKA RIα clone 18, anti-PKA RIIα clone 40, and anti-PKA RIIβ clone 45 were purchased from BD Biosciences (San Jose, CA, USA). Rabbit anti-PKA RIα (D54D9) was purchased from Cell Signaling (Danvers, MA, USA). GAPDH antibody (AM4300) was from Ambion (ThermoFisher Scientifics, Carlsbad, CA, USA). Alexa Fluor 594 or 647-conjugated α-Bungarotoxin, Alexa Fluor 488-conjugated, 594-conjugated, or 680-conjugated anti-mouse or anti-rabbit IgG were purchased from ThermoFisher Scientifics. Two mouse cTnT-specific shRNA TRCN0000120553, TRCN0000120555, and MISSION SHC002 control nontargeting shRNA were purchased from Sigma-Aldrich (St. Louis, MO, USA).

Animals, electroporation, and sciatic denervation

Animal housing and procedures were approved by the Animal Care and Use Committee of Wake Forest University Health Sciences. Limb muscles were dissected from male C57BL/6 or Friend virus B mice. We have used the latter strain previously as a model of ageing skeletal muscle. C57B16 mice were used for intramuscular plasmid injection and electroporation according to the techniques described by Files *et al.*[17] Briefly, skeletal muscle electroporation was carried out with a Grass stimulator (Grass S48; West Warwick, RI, USA) using platinum-coated paddles (Harvard Apparatus, Holliston, MA, USA). After removal of the animal's hair from the hindlimb and sedation with controlled isoflurane, 40 μL of bovine hyaluronic acid (0.3 U/μL in 0.9% NaCl; H3631-3KU Sigma-Aldrich, St Louis, MO, USA) was injected in 10 μL-aliquots up the length of the tibialis anterior (TA) muscle using a 26 gauge needle and syringe. Hyaluronic acid pretreatment prior to electroporation increases transfection efficiency. Two hours later, animals were sedated with isoflurane (2% inhaled at a constant flow rate of 2 L/min). The TA was then injected with 40 μL of plasmid encoding for cTnT targeting shRNAs (1 μg/μL plamid in 0.9% NaCl) in 10 μL-aliquots up the length of the muscle.

DOI: 10.1002/jcsm.12204

The contralateral leg was used as a control and injected with a plasmid encoding non-targeting shRNA (1 μg/μL plasmid in 0.9% normal saline). Immediately following plasmid injection, the muscle was electroporated with five 25 ms pulses of 150 V of electric current. At the time of harvest, TA muscle was cut in half longitudinally. One half was used for immunofluorescence staining and was fixed in 4% paraformaldehyde/phosphate buffered saline and prepared for sectioning and staining. The other half was frozen directly in liquid nitrogen for later RNA extraction. For sciatic nerve denervation of young mice, 5 mm of the sciatic nerve was removed from anaesthetized mice, which were sacrificed 14 days later for muscle RNA and protein analysis.

Vervet monkey and human muscle tissues

One vastus lateralis muscle biopsied from a 21-year-old (corresponding to humans in their 70s) African green vervet monkey was obtained from previously collected tissues[18] and used for protein expression assays. All procedures involving monkeys were conducted in accordance with state and federal laws, Department of Health and Human Services standards, and guidelines established by the Institutional Animal Care and Use Committee. In addition, a vastus lateralis muscle biopsy from a 72-year-old man collected previously[19] was used for protein expression assays. In addition, 10 more vastus lateralis muscle biopsies from pretreatment subjects in the SILVER trial (NCT01298817),[20] a study of using a soy-based meal replacement weight loss intervention to impact ectopic fat in obese older adults [1 man, 9 women, age: 66.6 ± 3.3 years; body mass index (BMI): 34.5 ± 4.5 kg/m^2], were used for RNA expression assays. The study was approved by the Wake Forest Institutional Review Board, and all participants signed informed consent to participate.

RNA isolation and expression analysis

Total RNA was extracted from muscle tissues using TRIZOL reagent (ThermoFisher Scientific) according to the manufacturer's instructions. To quantitatively analyse mRNA expression, 23.5 ng of total RNA was reverse transcribed into cDNA and amplified with the appropriate primers using a one-step kit (Lo-Rox Bio-78005 Bioline) and a thermo cycler (7500 fast real-time PCR system, Applied Biosystems) for real-time reverse transcription polymerase chain reaction (qRT-PCR) quantitation. Analysis was performed by the comparative threshold cycle (Ct) method under the following cycling conditions: 30 min at 45°C; 5 min at 95°C; 40 cycles of 10 s at 95°C, and 1 min at 60°C. Relative abundance of each mRNA was determined from the Ct values using the $2^{-\Delta\Delta Ct}$ method after normalization to GAPDH. All experiments were performed in triplicate. TaqMan probe-based primers (ThermoFisher Scientifics) were used in all reactions. Accession numbers are listed following each gene: Mouse *Tnnt2*, Mm01290256_m1; *Tnnt1*, Mm00449089_m1; *Tnnt3*, Mm01137842_g1; *chrng*, Mm00437419_m1; *Runx1*, Mm013404_m1; and GAPDH, Mm03302249_g1. Human *Tnnt2*, Hs00165960_m1; *Tnnt1*, Hs00162848_m1; *Tnnt3*, Hs00952980_m1; and GAPDH, Hs02758991_g1.

Protein extraction, electrophoresis, and immunoblotting

For immunoblotting, muscles were pulverized in liquid nitrogen and further homogenized using a bead blender (BBX24B Bullet Blue Blender, Next Advance) in Eppendorf tubes containing stainless steel beads (0.9–2.0 mm, Next Advance) and lysis buffer containing 60 mM Tris pH 6.8, 1% SDS, and 12% glycerol and then cleared by centrifugation. Protein concentrations were determined using a Bio-Rad DC protein assay kit (Hercules, CA, USA). Sodium dodecyl sulfate-polyacrylamide gel electrophoresis (SDS-PAGE) was conducted using a 4.5% stacking gel with a 14% resolving gel (180:1) in a mini-PROTEAN gel system (Bio-Rad Laboratories, Hemel-Hemptstead, Hertfordshire, UK) as previously described[16] or using mini-PROTEAN TGX,4–20% gradient gels from Bio-Rad. Gels were transferred to nitrocellulose membranes (Amersham Health, Little Chalfont, Buckinghamshire, UK) at 4°C overnight. Blots were blocked in 5% non-fat dry milk with 0.1% Tween-20 in Tris-buffered saline for primary antibody incubation. Specific proteins were detected with individual primary antibodies at 4°C overnight, and Alexa 680-conjugated secondary antibodies were used at a 1:10000 dilution at room temperature for 1 h. Band intensity was measured using an Odyssey imaging system (LI-COR Biotechnology, Cambridge, UK). Data are representative of three independent experiments. Western blot densitometry was carried out using Image J software (National Institutes of Health, Bethesda, MD, USA).

Immunoprecipitation of endogenous cardiac troponin T-protein kinase A R complexes from skeletal muscle

Skeletal muscle lysates were prepared using RIPA lysis buffer. The immunoprecipitation protocol was essentially as described previously[10] with slight modifications. Briefly, whole cell lysates from one piece of gastrocnemius muscle were prepared in radioimmunoprecipitation assay buffer [1% NP40, 0.5% sodium deoxycholate, and 0.1% SDS in 1× phosphate-buffered saline (PBS)] supplemented with complete mini-protease inhibitor cocktail (Roche) using stainless beads as described previously. The lysates were

DOI: 10.1002/jcsm.12204

combined with a 50% slurry of protein A/G agarose beads (Promega, Madison, WI, USA), and kept rotating for 4 h at 4°C to clear any protein that bound non-specifically to the beads. After removal of protein A/G agarose beads by centrifugation (1000 × *g*), the cleared supernatant was incubated overnight at 4°C with 10 μg 1C11 cTnT antibody or control mouse IgG. Antibody-cTnT complex was precipitated following incubation with protein A/G agarose beads for 1–2 h at 4°C. Beads were washed five times with Tris-buffered saline and 0.05% Tween-20, and bound material was eluted in SDS-PAGE sample buffer. Samples were boiled and separated by SDS-PAGE, transferred to nitrocellulose membranes and probed with cTnT, PKA RIα, and PKA RIIα antibodies, respectively.

Mass spectrometry analysis

To verify and confirm the specificity of cTnT protein expression in skeletal muscle, immunoprecipitated products using anti-cTnT antibody (1C11) were further analysed by mass spectrometry. Briefly, the samples were split in two aliquots and separated by 1D SDS-PAGE, one for western blot analysis to locate cTnT, and the other was stained with Coomassie blue R-250 (Bio-Rad, Hercules, CA, USA) to visualize the proteins in the gel and excise the cTnT band matching the cTnT location on the immunoblot. To avoid potential spill-over contamination from the neighbouring band, samples (10 μL each) were loaded into every other lane in a 10-well SDS-PAGE gel; each lane has a maximum loading volume of around 40 μL. The gel band was excised, and in-gel trypsin digestion was performed according to standard protocols. The resulting tryptic peptides were further separated and analysed by Dionex Ultimate 3000 nanoLC system (Thermo Scientific, Waltham, MA, USA) coupled to a Thermo Q Exactive HF mass spectrometer (Thermo Scientific, Waltham, MA, USA). A typical gradient was run for 90 min from 10% to 55% solvent B (80% acetonitrile, 20% H_2O, and 0.1% formic acid). Solvent A consisted of 5% acetonitrile, 95% H_2O, and 0.1% formic acid. The flow rate was set at 300 nL/min on an Acclaim PepMap RSLC (C18, 2 μm, 100 Å, 75 μm × 15 cm) analytical column (Thermo Scientific, Waltham, MA, USA). The mass spectrometer was operated in top 20 data-dependent mode. The peptide identification was then performed using the Sequest HT search engine in Protein Discoverer 2.1 and using the NCBI mouse database (Apr 2016) that provides isoform information.

Immunofluorescent staining and microscopy

After muscles were removed, they were embedded in tissue-freezing medium (Triangle Biomedical Sciences, Inc.) and frozen in liquid nitrogen. Tissue blocks were stored at −80°C until sectioning. For immunofluorescent staining, 12 μm longitudinal cryosections from young and old mice, or the ipsilateral and contralateral TA muscle from the same mouse, were mounted in parallel onto glass slides, so that the relative fluorescent signal strength and ratio between two groups are comparable. Briefly, mounted slices were fixed with 2% paraformaldehyde in PBS for 10 min and permeabilized with 0.5% Triton X-100 in PBS for 5 min at room temperature. After three washes with PBS, they were incubated for 1 h in blocking buffer (PBS with 10% normal goat serum (Vector Labs, Burlingame, CA)) and labelled with primary and secondary antibodies overnight at 4°C and 1 h at room temperature in a wet box, respectively. To allow the even staining of tissue, the blocking buffer and diluted primary and secondary antibodies were all covered with a piece of parafilm during incubation for even distribution of antibodies. Alexa Fluor 594 or 647-conjugated α-Bungarotoxin were incubated together with the secondary antibody. They were then mounted in HardSet Antifade Mounting Medium with DAPI (H-1500, Vector Lab). Wide-field immunofluorescence images were taken on an inverted motorized fluorescent microscope (Olympus, IX81, Tokyo, Japan) and an Orca-R2 Hamamatsu CCD camera (Hamamatsu, Japan). The camera driver and image acquisition were controlled with a MetaMorph Imaging System (Olympus) under the same parameters for each sample on the same slide. Digital image files were transferred to Photoshop 7.0 to assemble montages.

Compound muscle action potentials recording

Electromyographic recording of compound muscle action potentials (CMAPs) is a crucial *in vivo* method to determine neuromuscular transmission efficiency.[21] To assess NMJ transmission, we measured CMAPs in TA *in vivo* in anaesthetized mice following previously described procedures.[21,22] Briefly, mice were anaesthetized (2% inhaled isoflurane at a constant flow rate of 2 L/min and the ipsilateral (control shRNA) and contralateral (cTnT targeting shRNA) TA muscles were located. Muscles were then stimulated using intramuscular wire electrodes and repetitive maximal sciatic nerve stimulation (predetermined with a series of stimulation frequency for each individual TA muscle). The stimulation pulses (0.25-ms duration and 5-Hz frequency) were programmed using a Master-8 device (A.M. P. Instruments Ltd., Jerusalem, Israel). Electromyography signals were amplified by Bio Amp (AD Instruments, Colorado Springs, CO) and recorded on a computer with Chart 7 for Windows (AD Instruments) for offline analysis. For each individual TA muscle, the 3–5 highest maximum CMAP peaks were chosen for CMAP amplitude quantitation. Comparisons were carried out only between contralateral and ipsilateral TA muscles within each individual mouse.

DOI: 10.1002/jcsm.12204

Statistical analysis

Data analysis was performed with Prism 5.0 (Graphpad, La Jolla, CA). All data are presented as means ± SEM. An α-value of $P < 0.05$ was considered significant.

Results

Cardiac troponin T expression is increased in the skeletal muscle of old mice

To examine if cTnT is expressed higher in the skeletal muscle of older mice, we first compared cTnT mRNA levels in the skeletal muscle of young and old mice from two different strains (C57BL/6 and Friend virus B). In both strains, cTnT mRNA expressed higher in the skeletal muscle of old mice compared with younger controls (*Figure* 1A and Supporting Information *Figure* **S1**). As a positive control, gastrocnemius muscle from sciatic denervated young C57BL/6 mice also showed highly increased cTnT mRNA expression level compared with old mice (*Figure* 1A). Next, we examined and compared the protein levels of cTnT between young and old mice. Using whole muscle lysates from young mouse heart, gastrocnemius from young mice, and sciatic denervated young mice, we first performed immunoblot analysis with two different cTnT antibodies. 1C11 detected cTnT highly specifically in the immunoblot assay in lysates from heart and sciatic denervated muscles but not in the young muscle (*Figure* 1B). Similar results occurred with antibody 4B8 (*Figure* 1B), which was highly specific for cTnT in our previous study.[16] Further immunoblots using 1C11 antibody to compare cTnT protein expression levels in the gastrocnemius muscles of old vs. young mice revealed that both old and sciatic denervated skeletal muscle have relatively high cTnT protein expression than young mice (*Figure* 1B–C). In addition, immunoblots with 4B8 antibody detected cTnT protein expression in old tissues across species, including mice, vervet monkeys, and human beings (*Figure* 1D). Although both antibodies also detected some non-specific bands in the immunoblots, they were mostly distant from the cTnT bands around the 37 kDa region (Supporting Information *Figure* **S2**).

To further verify the presence of cTnT in old skeletal muscle and the specificity of cTnT antibodies, we first performed immunoprecipitation assays using whole muscle lysates from young mouse heart and compared 1C11 and 4B8 antibodies; 1C11 more efficiently immunoprecipitated endogenous cTnT (*Figure* 2A). We thus chose the 1C11 antibody and further immunoprecipitated cTnT from whole cell lysates from old TA muscle (*Figure* 2B). 1C11 immunoprecipitation products from old TA muscle were further analysed with mass spectrometry (see Materials and methods section). cTnT peptide fragments from skeletal muscle detected by mass spectrometry were matched to mouse cTnT (*Figure* 2C,D), and the detected peptide sequence are shared by all cTnT splicing forms (Supporting Information *Figure* **S3**). Importantly, neither TnT1 (slow muscle isoform) nor TnT3 (fast muscle isoform) was detected. In addition, in the 1C11 immunoprecipitation products, peptides matching to several other proteins with higher percentage of sequence coverage were also detected, most of which are skeletal muscle, but not cardiac muscle abundant proteins (Supporting Information *Table* **S1**). Noticeably, three of those proteins (tropomyosin alpha-1 chain, tropomyosin beta chain, and creatine kinase M-type) are known cTnT interacting partners in a yeast two-hybrid assay[10] and therefore could have been co-immunoprecipitated with cTnT. These data strongly support that (i) cTnT protein is expressed in the skeletal muscle of old mice; and (ii) 1C11 antibody detects cTnT in the skeletal muscle specifically and efficiently. In addition, the aforementioned data also revealed higher mRNA and protein expression levels of cTnT in the skeletal muscle of old mice compared with the young.

Cardiac troponin T is enriched at the neuromuscular junction region mainly in the fast skeletal muscle of old mice

Although expressed in the skeletal muscle of old mice, compared with the other two skeletal muscle TnT isoforms, cTnT comprises only a very small portion of the total TnTs, even at the mRNA level (Supporting Information *Figure* **S4**). Therefore, it is important to determine the subcellular localization of cTnT in the skeletal muscle for a better understanding of its potential biological role in old skeletal muscle. Given that cTnT functions as a D-AKAP that interacts with PKA RI and RII regulatory subunits,[10] both of which are enriched at the NMJ in skeletal muscle,[11–15] we next wanted to determine if cTnT is also localized at the NMJ. To test this, we performed double immunofluorescence staining using 1C11 anti-cTnT antibody to label endogenous cTnT and Alexa 568-conjugated α-bungarotoxin to label nicotinic acetylcholine receptors (nAChRs) at the postsynaptic NMJ membrane. Although cTnT was not detected at the NMJ in the slow soleus (SOL) or fast TA muscle from young mice, it was highly enriched at the NMJ in the TA but barely detected in the SOL from older mice (20–23 months old). NMJ localization of cTnT was confirmed by using three different mouse cTnT monoclonal antibodies (*Figure* 3) and a rabbit monoclonal antibody (Supporting Information *Figure* **S5**). The specific detection of endogenous cTnT at NMJ with four different antibodies strongly supports the enrichment of

DOI: 10.1002/jcsm.12204

Figure 1 Cardiac troponin T (cTnT) mRNA and protein expression in skeletal muscle of older adults. (*A*) qRT-PCR quantitation of cTnT in young (Y), old (O), and sciatic denervated young (Y-SCI) mouse gastrocnemius muscles. $^{**}P < 0.01$ ($n = 3$) compared with Y muscles. (*B*) cTnT protein expression in mouse heart (Hrt) and young (Y) and sciatic denervated (Y-SCI1, Y-SCI2) skeletal muscles. For 1C11 immunoblotting, 2 μg Hrt and 100 μg gastrocnemius muscle lysates were loaded; for 4B8 immunoblotting, 5 μg Hrt and 15 μg gastrocnemius muscle lysates were loaded. (*C*) 1C11 immunoblotting of cTnT in mouse heart, young, and old skeletal muscle. 2 μg Hrt and 100 μg gastrocnemius muscle lysates were loaded. (*D*) 4B8 immunoblotting of cTnT protein expression in old mouse gastrocnemius (m), vervet monkey vastus lateralis (mky), and human vastus lateralis (hu). Five-μg mouse heart lysates (hrt) were the positive control; Ponceau S staining of membrane shows even loading of 50 μg total skeletal muscle lysates.

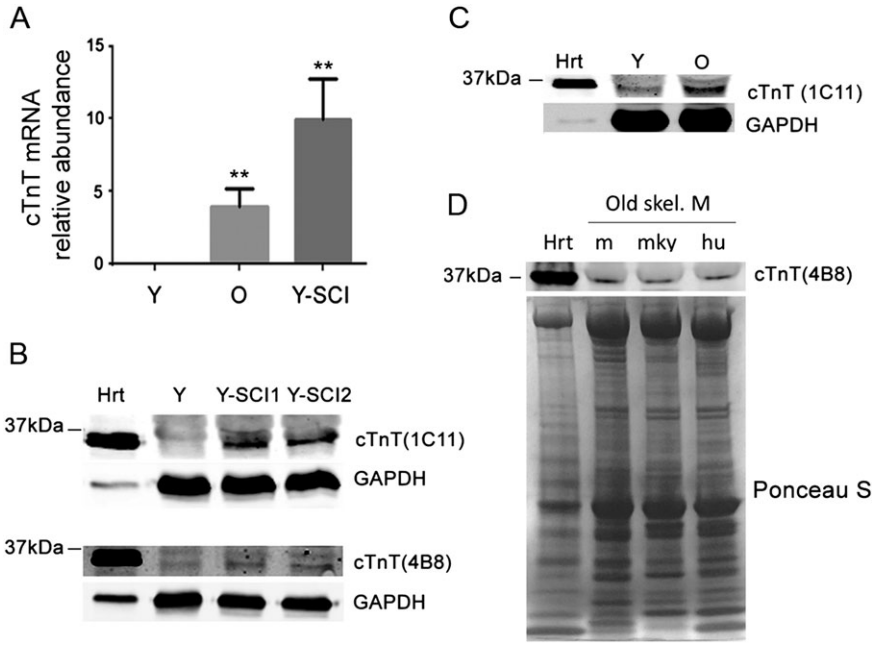

endogenous cTnT at NMJ in old fast TA muscles but not slow SOL muscles.

Protein kinase A RIIα, but not RIα, is enriched at neuromuscular junction in fast skeletal muscles of old mice

A sufficient number and density of nAChRs at the postsynaptic membrane adjacent to the motor neuron nerve terminal are crucial to maintain normal NMJ function, which could be regulated by postsynaptic PKA.[11–15] Because NMJ deteriorates in the fast skeletal muscle more severely with ageing than in slow skeletal muscle, while PKA RIα plays a key role in nAChR stabilization at the NMJ postsynaptic membrane,[12,15] we postulate that the amount of PKA RIα at the NMJ will decrease with ageing and possibly mainly in the fast skeletal muscles. To test this, we first performed double immunofluorescence staining of PKA RIα and NMJ in SOL and TA muscle cryosections from young and old mice. In fast TA muscle, PKA RIα was enriched at the NMJ in almost all young muscle samples but only in a few of the old muscle samples (*Figure* 4A). By contrast, PKA RIα was abundantly present at NMJ in SOL muscles from both young and old mice (*Figure* 4B). This finding was confirmed with two different previously well-characterized PKA RIα antibodies.[11,12] A third antibody simultaneously targeting PKA RIα/β (BD Biosciences) also failed to detect RI subunits at the NMJ in most TA muscle samples from old mice (data not shown).

Because rapsyn mediates subsynaptic anchoring of PKA type I and stabilization of nAChR *in vivo,*[15] we also compared rapsyn enrichment at the NMJ between young and old TA muscles; it was highly enriched at the NMJ in both old and young samples (Supporting Information *Figure* **S6**). We next analysed PKA RIIα at the NMJ. Although PKA RIIα was barely detected in the NMJ in TA of young mice (*Figure* 4C) or in SOL of young and old mice (*Figure* 4D), it was abundant in the NMJ in TA of old mice (*Figure* 4C). Furthermore, while both PKA RIIα and PKA RIIβ were detected at the NMJ in TA muscle of old mice, PKA RIIα was more abundant than RIIβ (*Figure* 4C and Supporting Information *Figure* **S7**). Both PKA RIα and RIIα were dispersed in muscle tissues beyond the NMJ area in young and old slow and fast skeletal muscles (Supporting Information *Figure* **S8**). To better quantify their protein expression levels, immunoblot data showed that the total muscle PKA RIα is expressed higher in slow SOL muscle than that in age-matched fast extensor digitorum longus (EDL)

DOI: 10.1002/jcsm.12204

Figure 2 Mass spectrometry determination of cardiac troponin T (cTnT) expression in skeletal muscle of old mice. (*A*) immunoprecipitation (IP) of cTnT from mouse heart lysates with control IgG, 1C11, and 4B8 antibodies. cTnT was detected with 1C11 antibody. Heart lysate was used as input control. HC, antibody heavy chain detected by secondary antibody. *(B)* IP of cTnT from old tibialis anterior (TA) muscle whole lysates with control IgG and 1C11. cTnT was detected with 1C11 antibody. Heart lysate and old TA lysate were used as input control. LC, antibody light chain detected by secondary antibody. IB, immunoblotting with 1C11. (*C*) Coomassie blue R-250-stained SDS-PAGE gels with separated IP products from heart and muscle lysates from old mice. Arrow indicates band of cTnT immunoprecipitated from heart lysates. The red box indicates location of cTnT from skeletal muscle. (*D*) Mass spectrometry of red boxed area on SDS-PAGE gel detected peptides from cTnT and several other skeletal muscle proteins (*Table* **S1**). Twenty one peptide fragments of mouse cTnT isoform g were detected, covering about 37% of the full-length cTnT protein sequence. SDS-PAGE, sodium dodecyl sulfate-polyacrylamide gel electrophoresis.

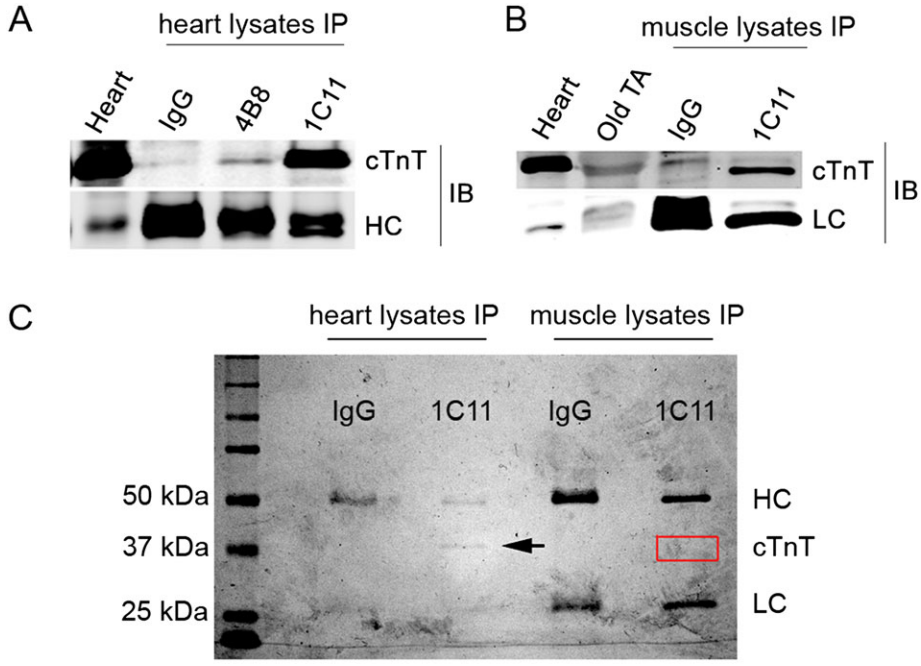

D

# Peptides	Protein IDs	Protein Name	Sequence Coverage (%)
21	NP_001123647	Troponin T, cardiac muscle isoform g	36.97

muscle (*Figure* 5A,B), while PKA RIIα increased with ageing in both SOL and EDL muscles (*Figure* 5A,C). Importantly, PKA RIIα/RIα ratio also increased with ageing in both EDL and SOL, with the relative ratio (set young SOL as 1) much higher in older fast EDL muscle than that in old SOL muscle (*Figure* 5A,D). The finding of PKA RIα and RIIα in not only the NMJ area but also in muscle fibres and fibre membranes is consistent with previous reports in the literature,[11,13] and this global expression and distribution pattern of PKA RIα and RIIα is consistent with the immunoblot findings. The aforementioned immunofluorescence staining and immunoblot data indicate that the total levels of PKA RIα and RIIα subunits, and their subcellular distribution, specifically at NMJ, may be differentially affected with muscle fibre type and age.

Because cTnT is a known D-AKAP[10] and is mainly enriched at NMJ in old fast skeletal muscle in our old mice model, we performed co-immunoprecipitation analysis to further examine cTnT-PKA RIα, RIIα complexes in gastrocnemius muscle from old mice. This is a fast-twitch skeletal muscle but contains both type II and type I muscle fibres[23] and therefore both PKA RIα and RIIα subtypes. Endogenous cTnT bound mostly to PKA RIIα in these gastrocnemius samples (Supporting Information *Figure* **S9**). A similar result was found in heart muscle from old mice (Supporting Information *Figure* **S10**). The higher binding affinity between cTnT and PKA RIIα in skeletal muscle of old mice may explain our finding that both cTnT and PKA RIIα are mainly enriched at the NMJ in old fast-twitch skeletal muscles (*Figures* 3 and 4C). Overall, these data indicate that PKA RIIα, but not RIα, is enriched preferentially at the NMJ in fast-twitch skeletal muscle of old mice, which may be regulated by binding with cTnT; it also indicates a potential role of cTnT in regulating NMJ function in old fast skeletal muscle through directly interfering with PKA signalling at that site.

DOI: 10.1002/jcsm.12204

Figure 3 Cardiac troponin T (cTnT) is highly enriched at the neuromuscular junction (NMJ), mainly in fast-twitch tibialis anterior (TA) skeletal muscle of old mice. Immunofluorescent staining of cTnT (green) with monoclonal antibody 1C11 and nicotinic acetylcholine receptor (nAChR) (red) with Alexa 594-conjugated bungarotoxin on longitudinal cryosections of young and old C57BL/6 soleus (SOL) and TA muscle. cTnT enrichment at NMJ in old TA was confirmed by two other mouse monoclonal antibodies (1F11 and 4B8) and one rabbit monoclonal antibody (*Figure* **S5**). Images are representative of five different young and old mice; in each mouse, at least 15 NMJs were analysed. Scale bar, 50 μm.

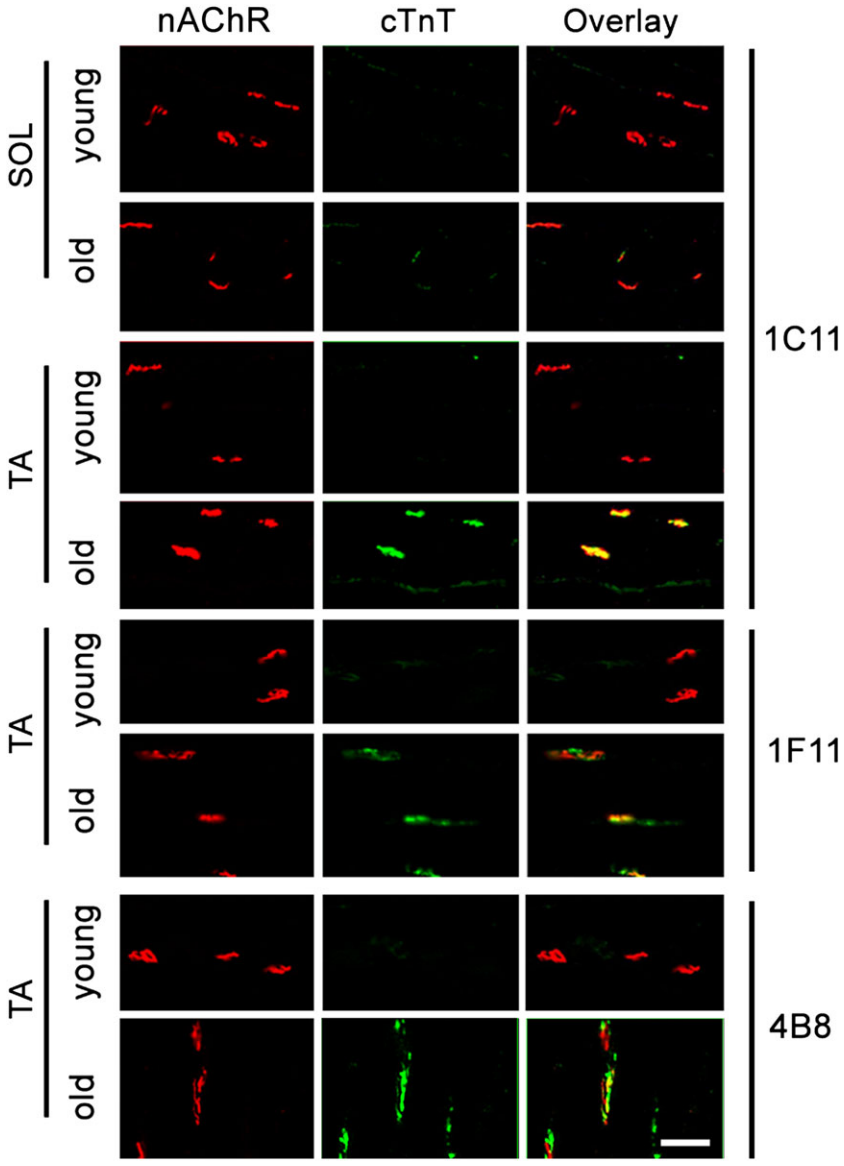

Cardiac troponin T down-regulation affects protein kinase A RIα, RIIα balance at the neuromuscular junction, reduces gene expression levels of muscle denervation markers, and improves compound muscle action potentials in old tibialis anterior muscle

If cTnT enrichment at the NMJ leads to increased PKA RIIα and decreased PKA RIα at that site, down-regulation of endogenous cTnT from NMJ should rescue PKA RIα and NMJ function. To further determine the role of endogenous cTnT at the NMJ in regulating PKA RIα, RIIα subunits, and NMJ neurotransmission, we performed a loss-of-function study by using two different shRNAs (sh_cTnT) to knock down endogenous cTnT in TA muscle of old mice. The ipsilateral TA (sh_cTnT electroporated) and contralateral TA (control sh_ctrl electroporated) were cut longitudinally after 14 days of electroporation. Subsequently, the efficiency of cTnT down-regulation was determined by immunofluorescence staining (*Figure* 6A) and qRT-PCR (*Figure* 6B). Gene expression levels of muscle denervation markers (*chrng* and *Runx1)* were significantly reduced in cTnT down-regulated

DOI: 10.1002/jcsm.12204

Figure 4 Protein kinase A (PKA) RIα and RIIα are differentially enriched at the neuromuscular junction (NMJ) in young and old tibialis anterior (TA) and soleus (SOL) muscle. Immunofluorescent staining indicated that (*A*) PKA RIα is enriched in most NMJs [nicotinic acetylcholine receptor (nAChR)-positive region] of young TA muscle and less so in old TA muscle; (*B*) PKA RIIα is enriched at the NMJ of both young and old SOL muscles, with a slight decrease in old SOL muscle; (*C*) PKA RIIα is not detected at the NMJ of young TA muscle yet is enriched in almost all NMJs in old TA muscle; (*D*) PKA RIIα is not detected at the NMJs of young SOL muscle and is detected only in a very small portion of NMJ in the old SOL muscles, with a much weaker signal compared with old TA muscles. Three mice in each group were analysed, with at least 15 NMJs counted in each mouse. $^{*}P < 0.05$; $^{****}P < 0.0001$. Scale bars, 50 μm.

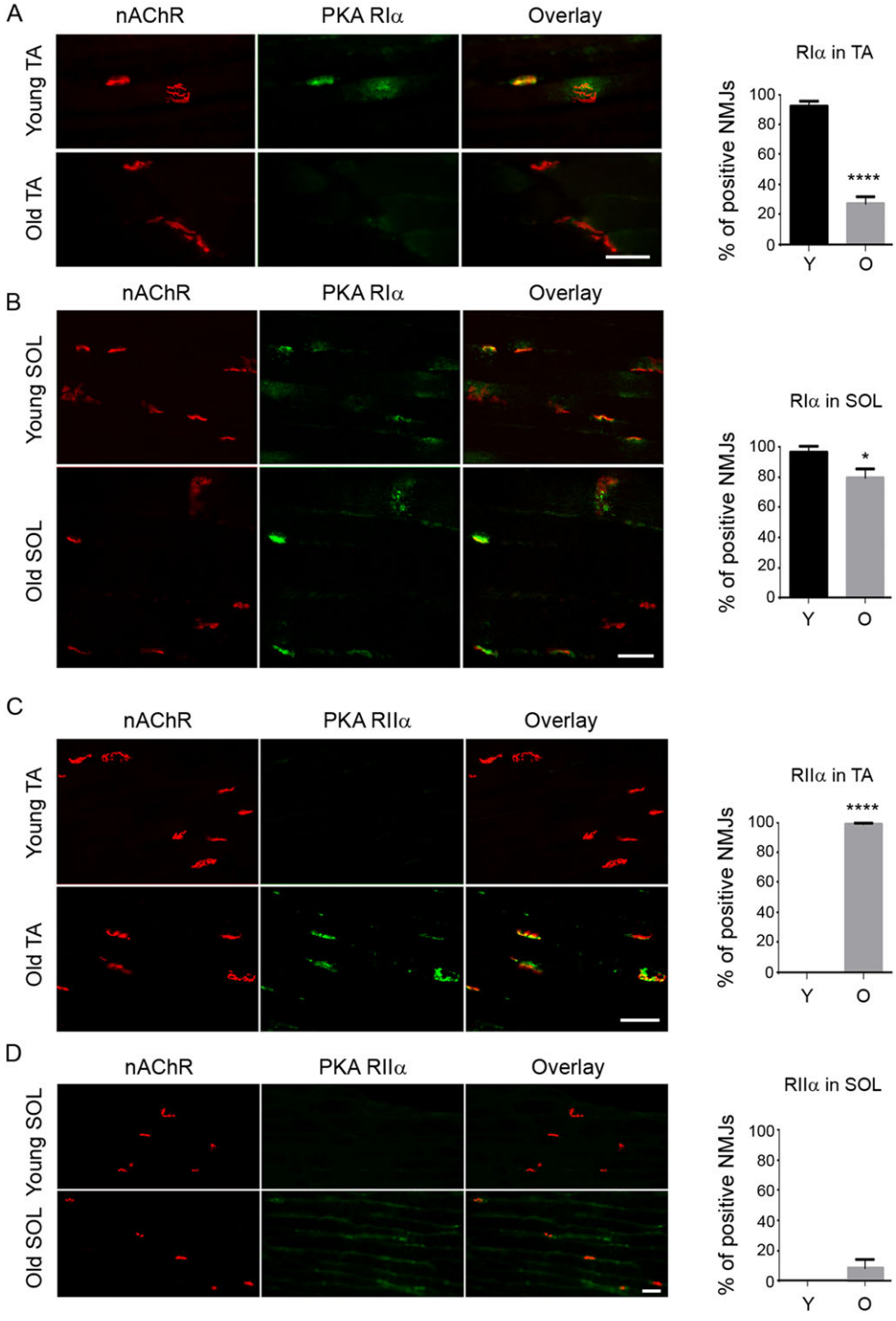

DOI: 10.1002/jcsm.12204

Figure 5 Protein kinase A (PKA) RIIα/RIα ratio increases more with ageing in fast extensor digitorum longus (EDL) muscle than in slow soleus (SOL) muscle. (*A*) Immunoblots of PKA RIα and RIIα in young and old EDL and SOL muscle lysates. GAPDH was used as a loading control. (*B–D*) PKA RIα, RIIα, and RIIα/RIα ratio after normalization with GAPDH. Y, young; O, old.*$P < 0.05$; **$P < 0.01$; ***$P < 0.001$ (n = 5).

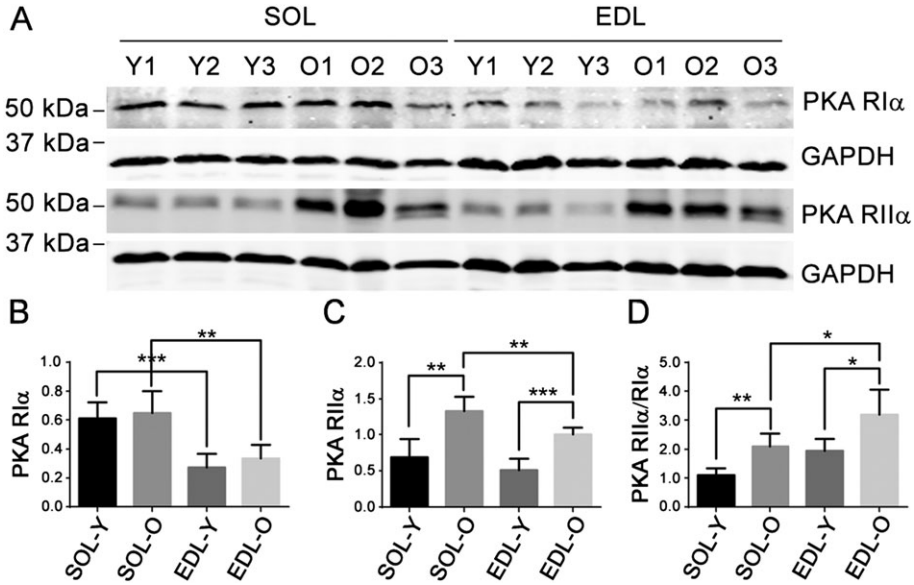

old TA muscles (*Figure* 6C,D). Down-regulation of these markers is closely related to cTnT knockdown, because at day 7 after electroporation, cTnT was not knocked down effectively, and neither were *chrng* nor *Runx1* (Supporting Information *Figure* **S11**). PKA RIα was elevated, while PKA RIIα was reduced at the NMJ area in cTnT down-regulated TA muscles (*Figure* 7). These data, together with the co-immunoprecipitation data, strongly indicate that cTnT at the NMJ contributes to PKA RIIα enrichment at NMJ in old TA muscle, which may competitively reduce PKA RIα at NMJ. Consequently, TA muscle with cTnT knocked down showed increased amplitude of CMAPs (*Figure* 8), which is a crucial *in vivo* method to determine neuromuscular transmission efficiency.[21,24,25] Altogether, our data suggest that down-regulation of cTnT at the NMJ may displace PKA RIIα from the NMJ and rescue RIα enrichment at that site, leading to enhanced NMJ function in muscle *in vivo*.

Discussion

Sarcopenia—age-related decline in skeletal muscle mass and function—is associated with physical disability, injuries, and death. It decreases quality of life in older adults and renders an increasingly heavy burden on the healthcare system. Ageing skeletal muscle undergoes chronic denervation, and the NMJ, the key structure that connects motor neuron nerves with muscle cells, shows increased deterioration in structure and function with ageing.[26,27] Previous studies have shown that with ageing, type II fast-twitch skeletal muscle fibres atrophy more than type I slow-twitch fibres across multiple species.[28–30] In addition, with ageing, NMJs are more vulnerable in fast-twitch skeletal muscle fibres than in slow-twitch skeletal muscle,[31–33] but it is unclear why. Understanding the key mechanisms regulating fast skeletal muscle fibre-specific denervation at the NMJ could be critical to identifying novel treatments for declines in muscle mass, force, and function in older adults.

In the current study, we demonstrated that (i) levels of cTnT expression and enrichment at the NMJ in skeletal muscle increase with ageing. In addition, cTnT enriched at the NMJ region with ageing is mainly in the fast-twitch, not the slow-twitch, muscle of old mice; (ii) in old mice, the PKA RIα subunit is largely removed from—while PKA RIIα and RIIβ are enriched at—the NMJ, again, preferentially in fast-twitch but not slow-twitch muscle in old mice; (iii) the PKA RIIα/RIα ratio increased with ageing and is higher in old fast-twitch muscle than slow-twitch muscle; (iv) cTnT forms complexes mainly with PKA RIIα in old fast skeletal muscle. Most importantly, knocking down cTnT in fast-twitch skeletal muscle of old mice (i) increased PKA RIα and reduced PKA RIIα at the NMJ; (ii) decreased the levels of gene expression of muscle denervation markers *chrng* and *Runx1*; and (iii) enhanced neurotransmission efficiency at NMJ. Together with the fact that cTnT can function as a D-AKAP,[10] our study provides the first evidence that cTnT plays a key role in regulating PKA signalling at the NMJ, and subsequently NMJ function, in an age-dependent and fast-twitch fibre-specific manner.

DOI: 10.1002/jcsm.12204

Figure 6 Gene expression levels of muscle denervation markers are inhibited by cardiac troponin T (cTnT) down-regulation by shRNA electroporation in old tibialis anterior (TA) muscle. Ipsilateral TA muscle was electroporated with cTnT-targeting shRNAs (sh_cTnT); the contralateral TA muscle was electroporated with control shRNA (sh_ctrl). (*A*) Representative immunofluorescent images indicate that 14 days after electroporation, cTnT was largely down-regulated at the neuromuscular junction [nicotinic acetylcholine receptor (nAChR)-positive area] in sh_cTnT electroporated TA muscle. qRT-PCR analyses of total RNA from each TA muscle indicate that cTnT mRNA was down-regulated by (*B*) sh_cTnT, whereas (*C*) *chrng*, and (*D*) *Runx1* were down-regulated in sh_cTnT electroporated TA muscle. Two different sh_cTnTs (see section) were tested in four mice. ***$P < 0.001$; ****$P < 0.0001$ ($n = 4$). Scale bar, 50 μm.

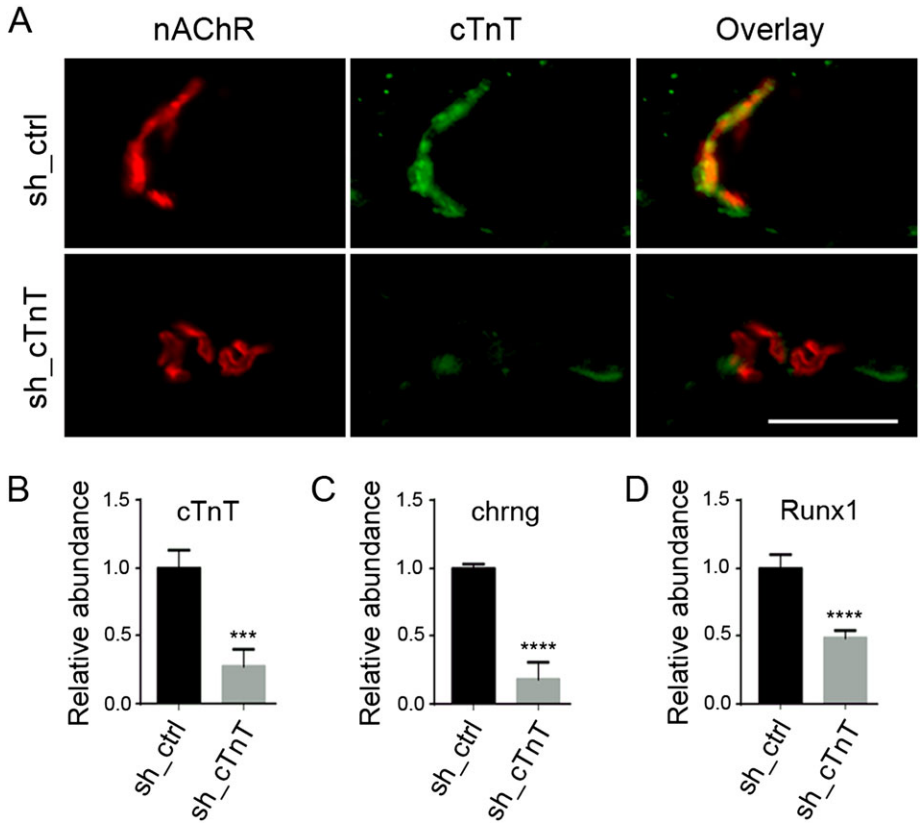

Cardiac troponin T is expressed in the skeletal muscle under various myopathic conditions, including denervation and neuromuscular diseases, and could be released into the circulation in those conditions.[8,34] Although the evidence collectively indicates cTnT as a potential biomarker of skeletal muscle denervation and/or regeneration, its role is still not clear. Our findings in old mice indicate that cTnT is expressed in the skeletal muscle and increases with ageing and contributes to NMJ functional decline in ageing muscle. Expression of cTnT in skeletal muscle was detected by immunoblot using two different antibodies, 1C11 and 4B8, with the latter well characterized in our previous publication.[16] The specificity of cTnT immunoprecipitated by 1C11 antibody from old fast skeletal muscle was further confirmed with mass spectrometry, yielding direct evidence that cTnT is highly specifically expressed in old skeletal muscle. In addition, 1C11 antibody specificity for cTnT was also confirmed, given that neither TnT1 nor TnT3 was detected in the immunoprecipitated cTnT-complex by mass spectrometry. Notably, mass spectrometry did not detect the unique peptide sequence of embryonic cTnT form but only detected the common regions that are shared among all cTnT splicing forms. This is consistent with previous observations that cTnT expressed in adult skeletal muscle during injury and regeneration is in the adult splice form, and the embryonic splicing pathways have been turned off in adult muscle.[35] Our finding further indicates that the expression of cTnT in ageing skeletal muscle is fibre type-dependent and is most possibly regulated by a fast-twitch fibre-specific environment. Yet because the NH2-terminal regional plays a key regulatory role for cTnT structure and function, it is important to further determine the exact cTnT splicing form in old skeletal muscle in future work.

To our knowledge, this is the first report showing that the ratio of RIIα/RIα in whole muscle changes differently with ageing in slow and fast skeletal muscles. It is also the first report documenting that their relative abundance at NMJ region also changes differently with ageing in slow and fast

DOI: 10.1002/jcsm.12204

Figure 7 Cardiac troponin T (cTnT) down-regulation led to increased protein kinase A (PKA) RIα and decreased RIIα enrichment at the neuromuscular junction (NMJ) in tibialis anterior (TA) muscle of old mice. Fourteen days after shRNA electroporation, sh_cTnT electroporated TA muscle shows (*A*) increased PKA RIα enrichment at NMJ [nicotinic acetylcholine receptor (nAChR)-positive area] and (*B*) decreased PKA RIIα enrichment at the NMJ. Most NMJs had fainter immunofluorescent signalling for PKA RIIα. Four mice were analysed with at least 15 NMJs counted in each mouse. ***$P < 0.001$; ****$P < 0.0001$. Scale bars, 50 μm.

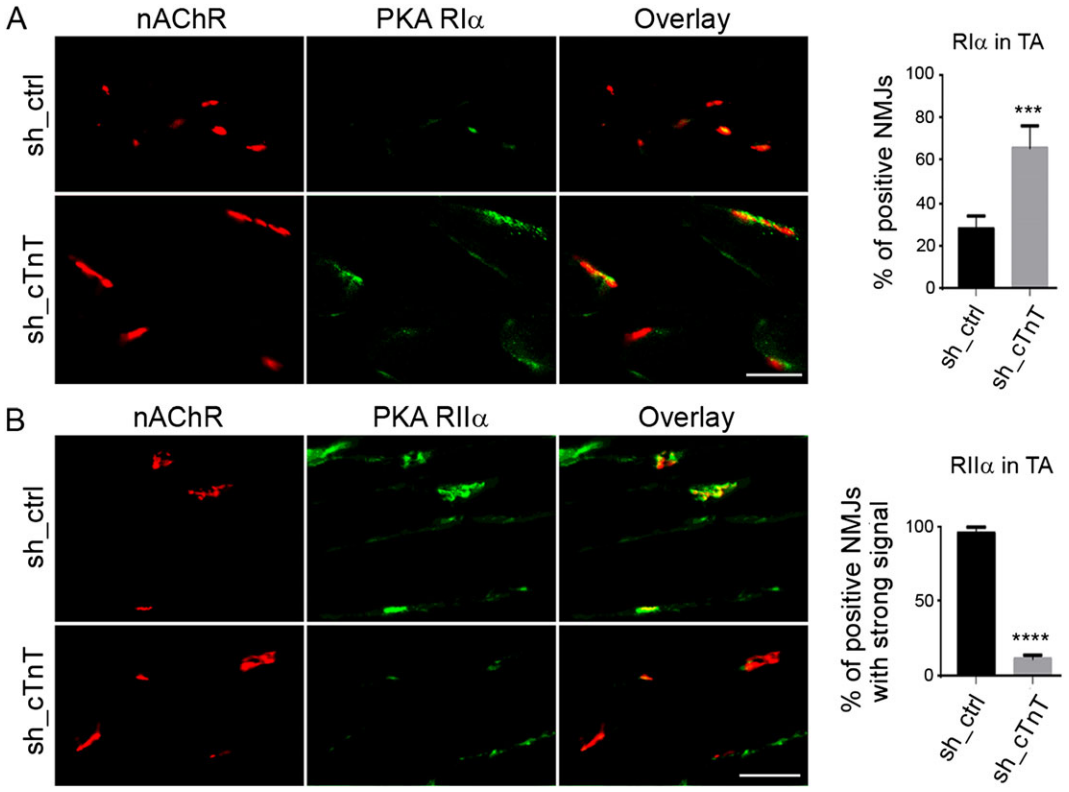

Figure 8 Cardiac troponin T (cTnT) down-regulation led to increased maximum amplitude of compound muscle action potentials (CMAP) in old tibialis anterior (TA) muscle. (*A*) Representative recordings in contralateral and ipsilateral TA 14 days after electroporation of sh_cTnT or sh_ctrl, respectively. (*B*) Fold changes in CMAP between contralateral and ipsilateral TA muscles in each mouse. The mean maximum CMAP amplitude in sh_ctrl electroporated TA muscle was set as '1' in each mouse. *$P < 0.05$ ($n = 4$).

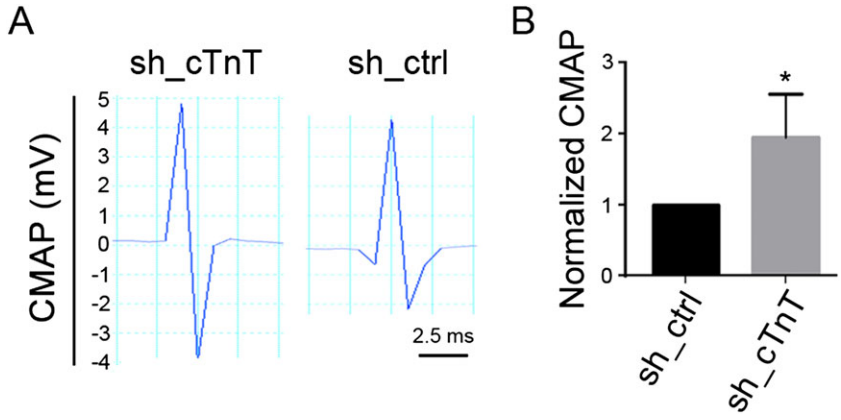

skeletal muscles. We also show that enrichment of PKA RIα and RIIα at NMJ could be regulated in a highly restrictive and spatially specific manner, which is regulated by cTnT. Previous work indicated that cTnT functions as a D-AKAP that interacts with the PKA regulatory subunits RI and RII,[10] both of which are localized at the NMJ.[11,15] Although PKA RIα, RIIα,

DOI: 10.1002/jcsm.12204

and RIIβ are all localized at the postsynaptic NMJ, their patterns differ.[11] The role of RIα in mediating nAChRs stabilization at the postsynaptic NMJ is known, but the role of RIIα and RIIβ at this site is still unknown.[12–15] Our data show for the first time that enrichment of PKA RIα and RIIα at NMJ is muscle type-specific and age-dependent, with PKA RIα mainly abundant at the NMJ in young muscle fibres and old slow-twitch fibres, while PKA RIIα was predominantly enriched at the NMJ in old fast-twitch fibres.

Our findings also indicated that cTnT preferentially binds PKA RIIα at the NMJ of old fast skeletal muscle fibres. This result is consistent with previous work. Although over 40 AKAPs have been discovered, most demonstrate specificity towards the PKA-RII isoform. Furthermore, although cTnT is a D-AKAP that binds to both RII and RI,[10] other D-AKAPs (e.g. D-AKAP1 and D-AKAP2) usually preferentially bind to RII,[36] as does cTnT in the heart muscle.[10] Our co-immunoprecipitation data in the old skeletal muscle also support a potentially higher binding affinity between cTnT and PKA-RIIα. The fact that cTnT and PKA RIIα are more abundantly enriched, yet PKA RIα is greatly reduced, at the NMJ in old fast-twitch skeletal muscle further indicates that, at least in the NMJ area, cTnT preferentially binds to PKA RIIα. Finally, we found that knocking down cTnT from the NMJ in TA muscle of old mice reduced PKA RIIα and increased PKA RIα at that site.

Multiple factors may have contributed to the preferential binding between cTnT and PKA RIIα at the NMJ. For instance, PKA RI appears to have a weaker binding affinity to the AKAP (s) compared with PKA RII; therefore, it could be released more easily from its binding site[37] In other words, the docking of RII is more static, whereas the docking of RI is more dynamic. In addition, RII subunits are typically localized to discrete sites in the cell, such as plasma membrane and cytoskeleton, while RI subunits tend to be more diffuse.[38] Our findings of the change in the relative abundance of RIIα and RIα or RIIα/RIα ratio with ageing in muscle and at the NMJ suggest that an increased RIIα/RIα ratio may subsequently favour enhanced cTnT and PKA-RIIα interaction, specifically at the NMJ in old skeletal muscle fast muscle fibres. Other ageing-related factors and muscle fibre environments (slow vs. fast) should also be considered and explored in future work.

Previous studies have shown that PKA RIα—but not PKA RIIα and RIIβ—interact with nAChRs at the postsynaptic membrane.[12] Therefore, cTnT enrichment at the NMJ in old skeletal muscle may competitively bind more PKA RII but less RI at the NMJ, subsequently inhibiting the PKA RIα signalling that mediates nAChRs stabilization at the postsynaptic NMJ. Given that myosin Va[12] and rapsyn[15] are involved in PKA RIα signalling at the NMJ, we examined both of them in this study. However, we saw no differences in rapsyn enrichment at the NMJ in old TA muscle, indicating that cTnT mediates PKA RI and RII binding at the NMJ in a rapsyn-independent manner. For myosin Va, we did not detect any signal in our immunofluorescence assay (data not shown), which could be limited by the sensitivity of antibody we used or the relatively small amount of endogenous myosin Va at NMJ.

Importantly, knocking down cTnT from NMJ in TA muscle of old mice reduced PKA RIIα and increased PKA RIα at that site, which consequently led to reduced levels of muscle denervation (*chrng* and *Runx1* gene expression), and improved neurotransmission, indicated by increased amplitude of CMAPs. Because decline in muscle denervation gene expression was not achieved at day 7 post-electroporation (when cTnT was not efficiently knocked down), down-regulation of denervation markers and up-regulation of CMAPs at day 14 post-electroporation appear to be directly or indirectly mediated through cTnT down-regulation. Because neurotransmission also plays a key role in nAChR stability at the postsynaptic NMJ membrane,[39] effects of cTnT down-regulation on rescue of CMAPs amplitude could be mediated through enhanced nAChR stability at NMJ, which is directly regulated by PKA RIα signalling. Future studies of nAChR dynamics and stability analyses will be critical to understand the detailed mechanisms. Because morphologic changes in the NMJ (e.g. fragmentation and degradation) are also common in ageing human and rodents and are related to muscle denervation, the effects of cTnT down-regulation on rescue of neurotransmission could also have been achieved through improved NMJ integrity, a target of future studies. Although presynaptic motor neuron nerve retraction is also involved in muscle denervation with ageing, only 13–15% of fast-twitch EDL or TA muscles are fully denervated in C57BL/6 mice at 24 months old.[31,40] We and others have also reported that only ~35% of endplates are partially denervated in the limb muscles of 21- to 24-month-old mice.[40,41] Because PKA RIIα was enriched and PKA RIα was reduced in almost all NMJs with positive cTnT in old TA, our cTnT shRNA knockdown study strongly supports the idea that targeting postsynaptic proteins involved in NMJ signalling could be useful to improve NMJ function. In line with this idea, it was recently reported that DOK-7 gene therapy effectively improved NMJ size and motor activity.[42]

In summary, our finding revealed for the first time that cTnT contributes to fast skeletal muscle NMJ function decline with ageing and further indicated that cTnT-PKA signalling could be a novel therapeutic target to improve NMJ function in the fast skeletal muscle of older mice. Given that fast skeletal muscles are more affected with ageing than slow skeletal muscles across species and cTnT protein is expressed in old skeletal muscle across species found in this study, our finding will provide strong evidence on development of future translational strategies for improving muscle function decline with ageing in human. Because NMJ structure and function deteriorates

DOI: 10.1002/jcsm.12204

and cTnT is elevated in the skeletal muscle in various neuromuscular diseases, for instance, Pompe disease[43] and amyotrophic lateral sclerosis,[44]cTnT could also be a potential therapeutic target for such diseases characterized by deteriorations in NMJ structure and function.

Acknowledgements

We thank Karen Potvin Klein, MA, ELS (Director of Grant Development and Medical Editing, Wake Forest Clinical and Translational Science Institute (CTSI; UL1TR001420; PI: McClain) for her editorial contributions to this manuscript.

This work was supported by a pilot grant (T.Z.) from the Wake Forest Claude D. Pepper Older Americans Independence Center (OAIC; P30AG21332) (S.K.) and a pilot grant (T.Z.) from the CTSI Ignition Fund; and from R01AG13934 (O.D.), and AR048816 (J.P.J.). The mass spectrometry analysis was performed by the Proteomics and Metabolomics Shared Resource supported by the Comprehensive Cancer Center of Wake Forest University grant (P30CA012197; PI: Pasche). The vervet monkey tissue was from P40 grant (OD010965). Medifast provided the meal replacements used in the SILVER study, which was supported by the Wake Forest OAIC and the Wake Forest University Translational Science Center. The authors certify that they comply with the ethical guidelines for publishing in the Journal of Cachexia, Sarcopenia and Muscle: update 2015.[45] [Correction added on 04 May 2017 after first online publication: the Acknowledgement section was amended to include the grant received for the vervet monkey tissue]

Online supplementary material

Additional Supporting Information may be found online in the supporting information tab for this article.

Figure S1. cTnT mRNA expression in skeletal muscle of Friend Virus B (FVB) mice increases with aging. cTnT mRNA expression in young (3 months) and old (26 months) *flexor digitorum brevis* (FDB) muscles by qRT-PCR. **, $p < 0.01$ ($n = 6$).

Figure S2. Full size immunoblot data for Figure B-D. Arrows point to cTnT bands detected with 1C11 or 4B8 cTnT antibody.

Figure S3. cTnT peptides sequences detected by mass spectrometry are common regions shared among all cTnT splicing forms. Sequence alignment of all cTnT splicing forms was performed using UniProt/Align. cTnT peptides sequences detected by mass spectrometry are highlighted in red boxes.

Figure S4. TnT isoform expression in old human and mouse skeletal muscles. (A) mRNA expression levels of all three TnT isoforms were measured by qRT-PCR using total RNA the from *vastus lateralis* (VL) muscle of older adults (n = 10, age = 66.6 ± 3.3, BMI = 34.5 ± 4.5) in SILVER study. (B) mRNA expression levels of all three TnT isoforms were measured by qRT-PCR using total RNA from young and old FDB muscle (n = 6) from Friend Virus B (FVB) mice. Y, young; O, old. **, $p < 0.01$; ***, $p < 0.001$; ****, $p < 0.0001$ vs. cTnT in young or old group, respectively; ##, $p < 0.01$ vs. Y-cTnT.

Figure S5. cTnT protein enrichment at the NMJ in skeletal muscle detected with a rabbit anti-cTnT antibody. Rabbit antibody from Abcam (ab125266) also detected cTnT at the NMJ (n-acetylcholine-positive region) in old mouse TA muscle. Scale bar, 50 μm.

Figure S6. Rapsyn enrichment at the NMJ in young and old TA skeletal muscle does not change. Immunofluorescent staining of rapsyn indicates that it is abundantly enriched at the NMJ (nAChR-positive region) in the TA muscle of young and old mice. Images are representative of 3 mice; at least 15 NMJs were analysed in each mouse. Scale bar, 50 μm.

Figure S7. PKA RIIβ enrichment at NMJ of old TA skeletal muscle. Immunofluorescent staining indicates that PKA RIIβ is enriched in most NMJs (nAChR-positive region) of old TA muscle, but not in young TA muscle. Compared to PKA RIIα in old TA muscle (see Figure), the PKA RIIβ signal is relatively weaker. Scale bar, 50 μm.

Figure S8. PKA RIα and RIIα global distribution among young and old TA and SOL muscles. Immunofluorescent staining revealed that in addition to their enrichment at NMJ area (indicated by overlay of nAChR and RIα or RIIα staining), both PKA RIα (A) and RIIα (B) were distributed in other areas beyond the NMJ region. The relative abundance of RIα and RIIα are comparable to that quantitated by immunoblot in Figure . Y, young; O, old. Scale bars, 50 μm.

Figure S9. Endogenously expressed cTnT interacts mainly with PKA RIIα in skeletal muscle of old mice. Old mouse gastrocnemius muscle lysates were used to immunoprecipitate endogenous cTnT-PKA RIα and RIIα complexes. cTnT binds preferentially to endogenous PKA RIIα, but not PKA RIα. Data shown are from a single experiment and representative of 3 separate experiments. IP, immunoprecipitation; IB, immunblot; HC, antibody heavy chain; NS, none specific band.

Figure S10. Endogenously expressed cTnT interacts mainly with PKA RIIα in heart muscle of old mice. Old mouse whole heart lysates were used to immunoprecipitate endogenous cTnT-PKA RIα and RIIα complexes. cTnT binds preferentially to endogenous PKA RIIα, but not PKA RIα. IP, immunoprecipitation; IB, immunblot; HC, antibody heavy chain.

Figure S11. cTnT down-regulation by shRNA electroporation in old TA muscle (7 days post-electroporation). On qRT-PCR, cTnT was not efficiently knocked down by cTnT targeting sh_cTnT compared to sh_ctrl. *Chrng* and *Runx1* were not

significant different between contralateral and ipsilateral TA muscles of old mice (n = 3).

Table S1. Mass spectrometry analysis of proteins purified through immunoprecipitation using cTnT antibody 1C11

Conflicts of interest

The authors declare that no potential conflicts of interest were disclosed.

References

1. el-Saleh SC, Warber KD, Potter JD. The role of tropomyosin-troponin in the regulation of skeletal muscle contraction. *J Muscle Res Cell Motil* 1986;**7**:387–404.
2. Asumda FZ, Chase PB. Nuclear cardiac troponin and tropomyosin are expressed early in cardiac differentiation of rat mesenchymal stem cells. *Differentiation* 2012;**83**:106–115.
3. Sahota VK, Grau BF, Mansilla A, Ferrus A. Troponin I and tropomyosin regulate chromosomal stability and cell polarity. *J Cell Sci* 2009;**122**:2623–2631.
4. Zhang T, Taylor J, Jiang Y, Pereyra AS, Messi ML, Wang ZM, et al. Troponin T3 regulates nuclear localization of the calcium channel Cavbeta1a subunit in skeletal muscle. *Exp Cell Res* 2015;**336**:276–286.
5. Zhang T, Pereyra AS, Wang ZM, Birbrair A, Reisz JA, Files DC, et al. Calpain inhibition rescues troponin T3 fragmentation, increases Cav1.1, and enhances skeletal muscle force in aging sedentary mice. *Aging Cell* 2016a;**15**:488–498.
6. Bodor GS, Survant L, Voss EM, Smith S, Porterfield D, Apple FS. Cardiac troponin T composition in normal and regenerating human skeletal muscle. *Clin Chem* 1997;**43**:476–484.
7. Rittoo D, Jones A, Lecky B, Neithercut D. Elevation of cardiac troponin T, but not cardiac troponin I, in patients with neuromuscular diseases: implications for the diagnosis of myocardial infarction. *J Am Coll Cardiol* 2014;**63**:2411–2420.
8. Saggin L, Gorza L, Ausoni S, Schiaffino S. Cardiac troponin T in developing, regenerating and denervated rat skeletal muscle. *Development* 1990;**110**:547–554.
9. Zhang SJ, Wang Q, Cui YJ, Wu W, Zhao QH, Xu Y, et al. High-sensitivity cardiac troponin T in geriatric inpatients. *Arch Gerontol Geriatr* 2016b;**65**:111–115.
10. Sumandea CA, Garcia-Cazarin ML, Bozio CH, Sievert GA, Balke CW, Sumandea MP. Cardiac troponin T, a sarcomeric AKAP, tethers protein kinase A at the myofilaments. *J Biol Chem* 2011;**286**:530–541.
11. Perkins GA, Wang L, Huang LJS, Humphries K, Yao VJ, Martone M, et al. PKA, PKC, and AKAP localization in and around the neuromuscular junction. *BMC Neurosci* 2001;**2**:17.
12. Roder IV, Choi KR, Reischl M, Petersen Y, Diefenbacher ME, Zaccolo M, et al. Myosin Va cooperates with PKA RIalpha to mediate maintenance of the endplate in vivo. *Proc Natl Acad Sci U S A* 2010;**107**:2031–2036.
13. Roder IV, Strack S, Reischl M, Dahley O, Khan MM, Kassel o, et al. Participation of myosin Va and Pka type I in the regeneration of neuromuscular junctions. *PLoS One* 2012;**7**:e40860.
14. Martinez-Pena y Valenzuela I, Pires-Oliveira M, Akaaboune M. PKC and PKA regulate AChR dynamics at the neuromuscular junction of living mice. *PLoS One* 2013;**8**:e81311.
15. Choi KR, Berrera M, Reischl M, Strack S, Albrizio M, Roder IV, et al. Rapsyn mediates subsynaptic anchoring of PKA type I and stabilisation of acetylcholine receptor in vivo. *J Cell Sci* 2012;**125**:714–723.
16. Feng HZ, Chen X, Hossain MM, Jin JP. Toad heart utilizes exclusively slow skeletal muscle troponin T: an evolutionary adaptation with potential functional benefits. *J Biol Chem* 2012a;**287**:29753–29764.
17. Files DC, D'Alessio FR, Johnston LF, Kesari P, Aggarwal NR, Garibaldi BT, et al. A critical role for muscle ring finger-1 in acute lung injury-associated skeletal muscle wasting. *Am J Respir Crit Care Med* 2012;**185**:825–834.
18. Feng X, Zhang T, Xu ZR, Choi SJ, Qian J, Furdui CM, et al. Myosin heavy chain isoform expression in the vastus lateralis muscle of aging African green vervet monkeys. *Exp Gerontol* 2012b;**47**:601–607.
19. Zhang T, Choi SJ, Wang ZM, Birbrair A, Messi ML, Jin JP, et al. Human slow troponin T (TNNT1) pre-mRNA alternative splicing is an indicator of skeletal muscle response to resistance exercise in older adults. *J Gerontol A Biol Sci Med Sci* 2014;**69**:1437–1447.
20. Beavers KM, Gordon MM, Easter L, Beavers DP, Hairston KG, Nicklas BJ, et al. Effect of protein source during weight loss on body composition, cardiometabolic risk and physical performance in abdominally obese, older adults: a pilot feeding study. *J Nutr Health Aging* 2015;**19**:87–95.
21. Khan MM, Lustrino D, Silveira WA, Wild F, Straka T, Issop Y, et al. Sympathetic innervation controls homeostasis of neuromuscular junctions in health and disease. *Proc Natl Acad Sci U S A* 2016;**113**:746–750.
22. Arnold WD, Sheth KA, Wier CG, Kissel JT, Burghes AH, Kolb SJ. Electrophysiological motor unit number estimation (MUNE) measuring compound muscle action potential (CMAP) in mouse hindlimb muscles. *J Vis Exp: JoVE* 2015;**103**:52899.
23. Bloemberg D, Quadrilatero J. Rapid determination of myosin heavy chain expression in rat, mouse, and human skeletal muscle using multicolor immunofluorescence analysis. *PLoS One* 2012;**7**:e35273.
24. Richman DP, Nishi K, Morell SW, Chang JM, Ferns MJ, Wollmann RL, et al. Acute severe animal model of anti-muscle-specific kinase myasthenia: combined postsynaptic and presynaptic changes. *Arch Neurol* 2012;**69**:453–460.
25. Plomp JJ, Morsch M, Phillips WD, Verschuuren JJ. Electrophysiological analysis of neuromuscular synaptic function in myasthenia gravis patients and animal models. *Exp Neurol* 2015;**270**:41–54.
26. Valdez G, Tapia JC, Lichtman JW, Fox MA, Sanes JR. Shared resistance to aging and ALS in neuromuscular junctions of specific muscles. *PLoS One* 2012;**7**:e34640.
27. Rudolf R, Khan MM, Labeit S, Deschenes MR. Degeneration of neuromuscular junction in age and dystrophy. *Front Aging Neurosci* 2014;**6**:99.
28. Ciciliot S, Rossi AC, Dyar KA, Blaauw B, Schiaffino S. Muscle type and fiber type specificity in muscle wasting. *Int J Biochem Cell B* 2013;**45**:2191–2199.
29. Nilwik R, Snijders T, Leenders M, Groen BBL, van Kranenburg J, Verdijk LB, et al. The decline in skeletal muscle mass with aging is mainly attributed to a reduction in type II muscle fiber size. *Exp Gerontol* 2013;**48**:492–498.
30. Larsson L, Ansved T, Edstrom L, Gorza L, Schiaffino S. Effects of age on physiological, immunohistochemical and biochemical properties of fast-twitch single motor units in the rat. *J Physiol* 1991;**443**:257–275.
31. Chai RJ, Vukovic J, Dunlop S, Grounds MD, Shavlakadze T. Striking denervation of neuromuscular junctions without lumbar motoneuron loss in geriatric mouse muscle. *PLoS One* 2011;**6**:e28090.
32. Vandervoort AA. Aging of the human neuromuscular system. *Muscle Nerve* 2002;**25**:17–25.
33. Balice-Gordon RJ. Age-related changes in neuromuscular innervation. *Muscle Nerve Suppl* 1997;**5**:S83–S87.
34. Jaffe AS, Vasile VC, Milone M, Saenger AK, Olson KN, Apple FS. Diseased skeletal muscle: a noncardiac source of increased circulating concentrations of cardiac troponin T. *J Am Coll Cardiol* 2011;**58**:1819–1824.
35. Jin JP. Alternative RNA splicing-generated cardiac troponin T isoform switching: a

non-heart-restricted genetic programming synchronized in developing cardiac and skeletal muscles. *Biochem Biophys Res Commun* 1996;**225**:883–889.
36. Herberg FW, Maleszka A, Eide T, Vossebein L, Tasken K. Analysis of A-kinase anchoring protein (AKAP) interaction with protein kinase A (PKA) regulatory subunits: PKA isoform specificity in AKAP binding. *J Mol Biol* 2000;**298**: 329–339.
37. Hoshijima M. Mechanical stress-strain sensors embedded in cardiac cytoskeleton: Z disk, titin, and associated structures. *Am J Phys Heart Circ Phys* 2006;**290**: H1313–H1325.
38. Wong W, Scott JD. AKAP signalling complexes: focal points in space and time. *Nat Rev Mol Cell Biol* 2004;**5**:959–970.
39. Avila OL, Drachman DB, Pestronk A. Neurotransmission regulates stability of acetylcholine-receptors at the neuromuscular junction. *J Neurosci* 1989;**9**:2902–2906.
40. Valdez G, Tapia JC, Kang H, Clemenson GD, Jr., Gage FH, Lichtman JW, et al. Attenuation of age-related changes in mouse neuromuscular synapses by caloric restriction and exercise. *Proc Natl Acad Sci U S A* 2010;**107**:14863–14868.
41. Wang ZM, Zheng Z, Messi ML, Delbono O. Extension and magnitude of denervation in skeletal muscle from ageing mice. *J Physiol* 2005;**565**:757–764.
42. Arimura S, Okada T, Tezuka T, Chiyo T, Kasahara Y, Yoshimura T, et al. Neuromuscular disease. DOK7 gene therapy benefits mouse models of diseases characterized by defects in the neuromuscular junction. *Science* 2014;**345**: 1505–1508.
43. Wens SC, Schaaf GJ, Michels M, Kruijshaar ME, van Gestel TJ, In 't Groen S, et al. Elevated plasma cardiac troponin T levels caused by skeletal muscle damage in Pompe disease. *Circ Cardiovasc Genet* 2016;**9**:6–13.
44. Mach L, Konecny T, Helanova K, Jaffe AS, Sorenson EJ, Somers VK, et al. Elevation of cardiac troponin T in patients with amyotrophic lateral sclerosis. *Acta Neurol Belg* 2016;**116**:557–564.
45. von Haehling S, Morley JE, Coats AJ, Anker SD. Ethical guidelines for publishing in the Journal of Cachexia, Sarcopenia and Muscle: update 2015. *J Cachexia Sarcopenia Muscle* 2015;**6**:315–316.

DOI: 10.1002/jcsm.12204